Intraretinal pigmented cells in retinal degenerative disease

Marina Yasvoina[1], Qian Yang[1], Sasha M. Woods[1], Tjebo F. C. Heeren[1,2], Grant M Comer[3], Catherine Egan[2], Marcus Fruttiger[1*]

1) University College London Institute of Ophthalmology, London, United Kingdom
2) Moorfields Eye Hospital NHS Foundation Trust, London, United Kingdom
3) W.K. Kellogg Eye Center, University of Michigan, Ann Arbor, USA
*Corresponding author, email: m.fruttiger@ucl.ac.uk

Financial support

This work was supported by the Lowy Medical Research Institute (LMRI), La Jolla, USA; TH received financial support from the LMRI. CE and MF are partially funded by the National Institute of health research (NIHR) Biomedical Research Centre for Ophthalmology, Moorfields Eye Hospital NHS Foundation Trust, London, United Kingdom. The views expressed are those of the authors and not necessarily those of the NHS, the NIHR or the Department of Health. The sponsor or funding organizations had no role in the design or conduct of this research.

Conflict of interest

No conflicting relationship exists for any author

Running title

Intraretinal pigmented cells

Author contribution

MY and MF designed the study, MY, QY, SMW contributed to data collection, data analysis and figure making, and all authors contributed to the interpretation of data and the writing and revision of the manuscript. MF is guarantor.

Synopsis

Invasion of the retina by pigmented cells may occur in several diseases.
Immunohistochemistry analysis of postmortem human tissue indicates that these cells are RPE derived and that not all invading cells are pigmented.

Abstract

Purpose: Invasion of pigmented cells into the retina occurs in retinal degenerative diseases, such as Macular Telangiectasia type 2 (MacTel) and Retinitis Pigmentosa (RP). These intraretinal pigmented cells may be derived from the retinal pigment epithelium (RPE), but differences and similarities between intraretinal pigmented cells and RPE have so far not been well characterised.

Design: Clinicopathologic case report.

Method: Here, we compared intraretinal pigment cells with RPE cells by immunohistochemistry. Immuno-histological stains for classic RPE markers (RPE65, CRALBP and KRT18) and blood vessels markers (lectin and collagen 4) were done on sections from postmortem eye tissue from two MacTel donors, an RP donor, and a control donor.

Main outcome measures: Presence of specific immunohistochemistry markers on intra retinal pigmented and RPE cells.

Results: We found that intraretinal pigmented cells did not express RPE65 and CRALBP, with a small subset expressing them weakly. However, they all expressed KRT18, which was also present in normal RPE cells. Interestingly, we also found clusters of KRT18 positive cells in the retina that were not pigmented.

Conclusions: Our findings suggest that RPE cells invading the retina de-differentiate (losing classic RPE markers) and can be pigmented or unpigmented. Therefore, the number of RPE cells invading the retina in retinal degenerative disease may be underappreciated by fundoscopy.

Key Message

- What is already known on this topic - Intraretinal pigmented cells are observed in several retinal diseases and are presumed to be RPE-derived. However, they usually do not express classical RPE markers, and no specific markers are known to date.
- What this study adds - Here we show in postmortem samples that intraretinal pigmented cells express the RPE marker KRT18. Furthermore, we also found KRT18 positive cells in the retina that were not pigmented.
- How this study might affect research, practice or policy – Our findings establish KRT18 as a novel marker for intraretinal RPE-derived cells, irrespective of their pigmentation status.

Introduction

Macular telangiectasia type 2 (MacTel) is an uncommon bilateral eye disease which can lead to central vision loss. Retinal alterations begin in a temporal paracentral area, eventually affecting a characteristic oval region centred on the fovea, the 'MacTel area' [1]. Although vascular alterations like ectatic capillaries and blunted vessels gave the condition its name, the disease is most likely of neurodegenerative character, with Müller cell loss across the MacTel area and smaller regions of photoreceptor loss [2,3]. During the early stages of the disease, clinical signs include retinal crystals and loss of both luteal pigment and retinal transparency. The appearance of dark, intraretinal pigmented patches tends to occur in more advanced disease stages, which is associated with outer retinal atrophy and complete loss of retinal sensitivity in this region [4].

In colour fundus images, the colour of the intraretinal pigment ranges from grey to black, depending on its location within the retina. It is often found in proximity to right angle vessels [5–8], can occur as solitary or multiple lesions, and can progressively increase in number and size [9,10]. The pigmentary plaques may be associated with retinal vessels invading the outer retina and subretinal neovascularisation lesions. These vascular abnormalities, which have also been linked to degenerative changes in the outer retina [11], may appear in OCT imaging as hyper-reflective spots. This OCT feature may also be based on intraretinal pigmented cells, which have been described in many other retinal diseases.

It has been suggested that the intraretinal pigmented cells are derived from hypertrophy and migration of retinal pigment epithelium (RPE) cells that have come into contact with retinal blood vessels and migrate along them [7]. A similar phenomenon has been described in retinitis pigmentosa (RP), where RPE cells migrate towards the retinal vasculature after loss of photoreceptors, eventually ensheathing the blood vessels and forming the clinically visible bone spicules [12,13]. Intra retinal pigmented cells have also been observed in cases of Leber congenital amaurosis [14], Best vitelliform macular dystrophy [15], and age-related macular degeneration (AMD) [16–18].. Here, we report the histological findings from two eyes with MacTel and compare them with an eye from a patient with RP, to provide further evidence of the nature of intraretinal pigmented cells in retinal degenerative disease.

Methods

Donor history

The study has ethical approval (UK National Research Ethics, IRAS project ID: 279162) and follows the tenets of the declaration of Helsinki. All donors documented their willingness to participate in the eye tissue donation programme of the study. Histological analysis was conducted on one eye each from 2 MacTel patients, one RP patient and two controls. MacTel donors 1 and 2 were participants of the MacTel natural history observation registry (NHOR). This means that after a clinical diagnosis of MacTel had been established, they were

consented before being enrolled into the registry study. At time of enrolment, the clinical diagnosis of MacTel was confirmed by the Moorfields Eye Hospital Reading Centre.

Donor 1 (MacTel case 1) had a history of diabetes mellitus type 2. Cause of death was a cerebrovascular accident in the seventh decade. Before death in April 2016, the left eye was additionally diagnosed with ocular ischemia due to near complete occlusion of the left carotid artery. Of note, there was no clinical evidence of diabetic retinopathy in either eye at the time of last examination in April 2016. Both eyes were obtained six hours and ten minutes postmortem at the Kellogg Eye Center, University of Michigan. The medical history of donor 2 (post-mortem delay before fixation was four hours) has been previously reported [2].

We compared the findings with the right eyes from a patient with RP and from two donors without a history of ocular disease. The three eyes were obtained from the Moorfields BioBank with ethical approval from the institutional board and ethics committee. The eye with RP (donor 3, cause of death bronchopneumonia in seventh decade) was obtained nine hours post-mortem. The eyes from donor 4 (unknown cause of death in eighth decade) and 5 (cause of death breast cancer in sixth decade) were obtained 18 and 22 hours post-mortem, respectively, and served as controls for immunohistochemistry. All eyes were fixed in 4% paraformaldehyde (PFA) after excision. Representative, haematoxylin and eosin-stained sections from MacTel case 1, the RP case and a control case are shown in a supplementary figure (**Fig. S1**).

Clinical Imaging

Colour fundus photography, fluorescein angiography (FFA), fundus autofluorescence (AF) and OCT images were obtained with the standard imaging protocol of the MacTel NHOR study [6] for MacTel donor 1.

Tissue Processing

In all cases, the central region of the right eye was dissected to include optic disk, fovea, nasal and temporal periphery. The sample from MacTel donor 1 was cryoprotected in 30% sucrose overnight, embedded in 10% carboxymethylcellulose, and snap frozen in iso-pentane at -100°C. The samples from the control cases (donors 4 and 5) were cryoprotected in 30% sucrose overnight, embedded in Optimal Cutting Temperature compound (Scigen) and snap frozen iso-pentane at -100°C. Cryosections were obtained from frozen tissue using a Leica CM1850 cryostat at 15µm in thickness and mounted on Leica slides. The samples from MacTel donor 2 and from donor 3 (RP) were dehydrated through a series of alcohols automatically processed by a LEICA TP1020 tissue processor (Leica, UK) and embedded in paraffin wax prior to cutting on a sledge microtome at 6 µm in thickness and mounted on Leica BOND™ Plus Slides (Leica, USA). Before immunohistochemistry,

paraffin sections were deparaffinized with xylene and rehydrated with a series of ethanol dilutions.

Immunofluorescence

Heat induced antigen retrieval was performed on paraffin sections by heating the slides to 120°C in 90 molecular grade glycerol and 10% of 0.01M citrate buffer (pH6.0) for 10 minutes. Sections were washed in ddH_2O and incubated in a blocking buffer of 1% bovine serum albumin (BSA) and 0.5% Triton-X100 in phosphate-buffered saline (PBS). Primary antibody was diluted in the blocking buffer and incubated at 4°C overnight. After three washes in PBS, sections were incubated with appropriate secondary antibody diluents for 2 hours at room temperature.

Potassium permanganate bleaching

Some sections were treated with potassium permanganate before immunohistochemistry to bleach melanin [19,20]. Sections were incubated in 1% aqueous potassium permanganate for 10 minutes and rinsed with ddH_2O. A 10% solution of oxalic acid was applied to slides for 3 minutes. The slides were rinsed with ddH_2O and incubated in PSB for 10 minutes at room temperature. Only slides used for IBA1/ASMA/collagen triple immunostaining and Lectin/KRT18 double immunostaining were bleached.

Antibodies

Primary antibodies used were: Alpha-smooth muscle actin (ASMA) (monoclonal, mouse anti-human, C6198, Sigma, dilution 1:500), aquaporin-4 (polyclonal, rabbit anti-human, NBP187679, Novus, dilution 1:500), CK18 (polyclonal, rabbit anti-human, 10830, Proteintech, dilution 1:500), collagen IV (polyclonal, rabbit anti-human, 2150-0140, Bio-Rad, dilution 1:500), retinaldehyde binding protein 1 (CRLBP1) (monoclonal, mouse anti-human, MA1-813, Thermo Fisher, dilution 1:300), Iba1 (polyclonal, rabbit anti-human, 019-19741, Wako, dilution 1:1000), RPE65 (monoclonal, mouse anti-human, MAB5428, EMD Millipore, dilution 1:500), Vimentin-Cy3 (monoclonal, mouse anti-human, C9080, Sigma, dilution 1:300), Rhodamine-conjugated Ulex Europaeus Agglutinin (RL-1062, Vector Labs, dilution 1:500). Secondary antibodies used were Donkey anti-Mouse IgG (H+L) Alexa Fluor® 555 (A31570, Invitrogen, dilution 1:300), Donkey anti-Rabbit IgG (H+L) Alexa Fluor® 488 (A21206, Invitrogen, dilution 1:300), Donkey anti-Rabbit IgG (H+L) Alexa Fluor® 647 (A31573, Invitrogen, dilution 1:300).

Microscopy

Widefield images were taken using Invitrogen™ EVOS™ FL Auto 2 (Thermo Fisher, UK) with 20X objective. Confocal images were taken using Zeiss LSM700 or LSM710 microscopes. For IBA1/ASMA/collagen triple immunostaining and Lectin/KRT18 double immunostaining, melanin granules were visualized with transmitted light in the EVOS (X200 magnification) after deparaffinization and before immunostaining. Slides then went through bleaching

steps and proceeded with immunofluorescent staining. Brightfield images were then orientated and overlaid with 70% transparency on top of corresponding confocal images. Otherwise, Zeiss LSM700 was equipped with a T-PMT (Transmission-Photomultiplier) to collect differential interference contrast (DIC) images of the melanin granules.

Results

Clinical description

Both eyes from donor 1 showed full thickness macular holes which is a rare feature in MacTel, with a recently reported prevalence in a MacTel study cohort of 1.7% [1]. Marked intraretinal pigment plaques were visible in the right eye on colour fundus images in 2006 and 2013 with a greyish hue, suggesting a position in inner retinal layers (**Fig. 1A**). In the left eye pigmentation was faint in 2006 but became more noticeable by 2013 (**Fig. 1A'**). A particularly large pigment plaque expansion could be seen in the nasal perifovea of the right eye where a blunted vessel was present near the plaque (**Fig. 1A**). Fluorescein angiography revealed vascular leakage in the centre of the macula in both eyes (Fig. 1B and B'). However, some of that signal might also be caused by a localised loss of RPE pigmentation or RPE cells (arrowheads), which reveals fluorescein in the underlying choroid vasculature (so called "window defect"). Corresponding dark grey patches in autofluorescence imaging (arrowheads in **Fig. 1C** and **C'**) and light patches in the colour fundus images (arrowheads in **Fig. 1A** and **A'**) further support the notion of localised RPE defects.

A post-mortem photograph of the right eye of donor 1, taken in 2016 (**Fig. 1D**), shows that the shape and size of the pigmented plaques remained relatively stable since 2013. The location of the macular hole (visible as light brown patch in **Fig. 1D**) and the distribution of the retinal vessels were used to match the clinical images with the histological sections. The dotted line in **Fig. 1D** shows the approximate location of the OCT B-scan in **Fig. 1E** and a brightfield image of a cryosection from that retinal region (**Fig. 1F**). The localisation of the three hyperreflective clusters seen in the OCT image (arrows in **Fig. 1E**) matches with the pigmented clusters seen in bright field microscopy of the cryosection (arrows in **Fig. 1F**). Clinical findings for donor 2 were previously reported [2] and similar to donor 1, but with only one (and a much smaller) intraretinal pigment plaque.

Blood vessels and Müller cells

To investigate the association between blood vessels and pigmented cells we used antibodies against collagen IV to stain for blood vessel basement membrane. Within the MacTel area (where Müller cells are lost), we found many vessels that morphologically appeared normal, but were associated with patches of pigmented cells containing densely packed melanin granules (**Fig. 2A, A')**, which is not seen outside the MacTel area (not shown) or in normal retina (**Fig. 2C**). Furthermore, in some vessels the basement membrane appeared thicker than normal and formed irregular collagen IV deposits not seen in retina of healthy donors (**Fig. 2D, D'**). Similarly, in the RP sample, pigmented cell clusters were

associated with collagen IV positive structures (**Fig. 2B, B', E, E'**). Immunostaining with antibodies against aquaporin 4 (AQP4, expressed by Müller cells) showed a few AQP4 positive remnants associated with the abnormally shaped vessel/pigment cluster in the MacTel sample (**Fig. 2D, D'**) but otherwise there was no evidence of Müller cells. In contrast, there was extensive AQP4 staining in the RP and control sample (**Fig. 2E, E', F**). Using antibodies against vimentin (**Fig. 2G-I**) also demonstrated that Müller cells keep a normal morphology in the control eye but undergo reactive gliosis in the RP eye and are almost absent in the centre of the MacTel eye.

RPE and pigmented cells

CRALBP is expressed in Müller cells and the RPE. Antibody staining against CRALBP showed that Müller cells were largely absent in the central retina in the MacTel sample, as previously reported [2,3] (**Fig. 3A**). In contrast, CRALBP positive RPE cells, were present across the entire retina (black arrowheads in **Fig. 3A**), with the exception of two patches (white arrowheads in **Fig. 3A**). Both of these patches were localised around clusters of vessels, collagen deposits and pigmented cells that reached to Bruch's membrane. The majority of pigmented cells (which were much more strongly pigmented than normal RPE) did not or only very weakly stain for CRALBP (**Fig. 3 A-C'**). At higher magnification it was also notable that autofluorescent lipofuscin and melanofuscin granules (a hall mark of human RPE cells) were visible in some CRALBP positive cells (arrowheads in **Fig. 3B, B'**), but absent in the darkly pigmented, CRALBP negative cells (arrows in **Fig. 3B-C'**). In the RP sample (**Fig. 3H-I'**), CRALBP staining revealed gliosis in the retina, but was absent from the darkly pigmented intraretinal cells.

It is possible that the presence of excessive melanin pigment in the intra retinal cells may have blocked fluorescent signals. We therefore used potassium permanganate to bleach melanin pigment [19,20]. Before the bleaching, the retina was imaged in brightfield to localise pigmented cells in the section (**Fig. 3D**). After bleaching, we used antibodies against RPE65, which is another marker for RPE cells [21,22]. RPE65 was strongly expressed in normal RPE (arrowhead in **Fig. 3D, E**) but bleaching of the pigment did not reveal any further stains and the pigmented clusters visible in **Fig. 3E-G** remained RPE65 negative except for very few weakly positive cells (**Fig. 3G**).

Since the majority of the darkly pigmented intraretinal cells did not express two classic RPE markers (CRALBP and RPE65) we wondered whether this could be due to epithelial-mesenchymal transition (EMT). It has been previously shown that RPE cells undergoing EMT downregulate RPE markers and begin to express mesenchymal proteins such as vimentin and alpha smooth muscle actin (ASMA) [23–27]. In the MacTel retina from donor 1, vimentin was expressed in Müller cells in the peripheral retina where they were present, but little vimentin immunoreactivity was detected in the central retina. Intra-retinal pigmented cells were not positive for vimentin (**Fig. 2G, G'**). Furthermore, ASMA was present only in

vascular smooth muscle cells as expected, but no immunoreactivity was detected in intra-retinal pigmented cells in the two MacTel retinas and the RP retina (**Fig. 4A-E**).

Next, we tested whether the darkly pigmented intraretinal cells might be phagocytic cells. Macrophages in the retina can appear hyperpigmented after phagocytosing melanosomes [28]. We therefore immunolabeled retina from Mactel patients, a RP patient and a healthy donor with antibody raised against microglial protein IBA. Both MacTel eyes, the RP eye and the control showed some IBA1 positive microglia distributed throughout the retina. Some were also found in close proximity or within the clusters of blood vessels and pigmented cells in both temporal and nasal perifovea. However, their distribution did not match the distribution of intra-retinal pigmented cells (**Fig. 4A-D**).

Melanin granules in RPE cells can easily be identified by light microscopy due to their large size. In comparison, choroidal melanocytes contain much smaller melanin granules. Interestingly, the melanin granules in the intraretinal pigmented cells in the MacTel and the RP sample match the size of those in RPE cell (**Fig. 4F-H**). This further supports the notion that the invading intraretinal cells in MacTel are – similarly to RP - derived from RPE. In summary, these results show that intraretinal-pigmented cells are neither derived from microglial or choroidal melanocytes nor do they express mesenchymal markers.

Despite intraretinal, darkly pigmented cells not expressing the two RPE-specific markers RPE65 and CRALBP, we wanted to further explore the notion that these cells are RPE derived. We therefore tested whether they express cytokeratin 18 (KRT18), which is specific to epithelial lineage cells [29]. In the eye, KRT18 expression is restricted to the RPE [30–33]. Importantly, hyperplastic RPE cells retain KRT18 expression in uveal melanoma, and cultured human RPE cells continue to express KRT18 [30,34]. Immunolabeling of MacTel retina with antibodies against RPE65 and KRT18 showed that RPE adjacent to Bruch's membrane co-labelled for RPE65 and KRT18, as expected (**Fig. 5A-C, E-G**). Furthermore, all intraretinal pigmented cells were also expressing KRT18 (**Fig. 5E'-G'**). Remarkably, within the pigmented clusters, even cells that were only weakly or not pigmented were KRT18 positive (arrowheads in **Fig. 5**). Interestingly, we made similar findings in a sample from an RP patient, where clusters of pigmented cells also contained non-pigmented cells that were KRT18 positive (arrowheads in **Fig. 5D, H, H'**).

Discussion

Here we showed that intraretinal pigmented cells in MacTel and RP do not express classic RPE markers such as RPE65, but that they are KRT18 positive. Furthermore, some intraretinal KRT18 positive cells were also non-pigmented. Since KRT18 is strongly expressed in normal RPE cells (and nowhere else in the retina), it is likely that all intraretinal KRT18 positive cells (pigmented and non-pigmented) are RPE derived.

Clinically, pigmentary changes in the retina are important signs because pigment is very conspicuous in fundoscopy; with both retinal diseases and conditions of the RPE itself associated with altered pigmentation. Alterations in pigmentation can be associated with diseased RPE cells and associated outer retinal atrophy, as in RPE hamartomas [35] or solitary congenital hypertrophy of the RPE [36]; or the cells can show normal morphology with normal overlying photoreceptors, as in grouped type of congenital hypertrophy or reticular degeneration of the RPE [37,38]. Pigmentary changes in RPE have also been described in other degenerative retinal diseases, for example age-related macular degeneration (AMD), where RPE cells have been reported to undergo phenotypic changes associated with migration and degeneration, including transdifferentiation[39,40] and changes to melanosome load [41].

Based on our description of RPE65 and CRALBP negative intraretinal pigmented cells, we hypothesise that when RPE cells migrate into the retina in MacTel or RP, they partially de-differentiate or trans-differentiate or transform. RPE cells are known to lose markers they normally express in in their fully differentiated state in response to stress or disease, often involving proteins that contribute to interactions between RPE and photoreceptors [26,42–44]. Furthermore, intraretinal pigmented cells with no RPE65/CRALBP expression have also been previously described in cases of AMD [16]. Similarly, in our samples we found that the majority of RPE cells that have invaded the retina lose both RPE65 and CRALBP expression but retained expression of KRT18.

Regarding pigmentation, we observed two distinct phenotypes since the intraretinal KRT18-positive clusters contained non-pigmented and very strongly pigmented cells. It is not clear from our data whether the nonpigmented KRT18 positive cells are precursors of the strongly pigmented KRT18 positive cells, or whether the relationship is the other way around. It is possible, however, that the strongly pigmented phenotype is induced by interactions with retinal blood vessels. Normal RPE cells need a basal membrane scaffold which is provided by the vasculature. The accumulation of RPE around blood vessels in MacTel results in similar vascular alterations as in RP: breakdown of the blood-retinal barrier and thickening of the basement membrane [12].

It is likely that pigmented, KRT18 positive cells contribute to hyperreflective spot/foci in OCT imaging in MacTel as it has been shown in other pathologies such as AMD [16] or Acquired Vitelliform Lesions [45]. It is also plausible that non-pigmented KRT18 positive cells are not completely transparent (like the rest of the retina) and by having light scattering properties, they may also contribute to the hyper reflective spot signal in OCT imaging. Whilst de-pigmentation is classically associated with cultured RPE cells [24,46,47] it has, to our knowledge, so far not been described in human tissues. Our results therefore demonstrate that invasion of RPE cells into the retina in MacTel may be underappreciated because not all invading cells are pigmented.

References

1. Heeren TFC, Chew EY, Clemons T, et al. Macular telangiectasia type 2 - Visual acuity, disease endstage and the MacTel Area. MacTel Project Report No. 8. Ophthalmology 2020.

2. Powner MB, Gillies MC, Zhu M, et al. Loss of Müller's cells and photoreceptors in macular telangiectasia type 2. Ophthalmology 2013;120:2344–2352.

3. Powner MB, Gillies MC, Tretiach M, et al. Perifoveal müller cell depletion in a case of macular telangiectasia type 2. Ophthalmology 2010;117:2407–2416. Available at: http://dx.doi.org/10.1016/j.ophtha.2010.04.001.

4. Charbel Issa P, Gillies MC, Chew EY, et al. Macular telangiectasia type 2. Prog Retin Eye Res 2013;34:49–77. Available at: http://dx.doi.org/10.1016/j.preteyeres.2012.11.002.

5. Balaskas K, Leung I, Sallo FB, et al. Associations between autofluorescence abnormalities and visual acuity in idiopathic macular telangiectasia type 2: MacTel project report number 5. Retina 2014;34:1630–6.

6. Clemons TE, Gillies MC, Chew EY, et al. Baseline characteristics of participants in the natural history study of macular telangiectasia (MacTel) MacTel project report No. 2. Ophthalmic Epidemiol 2010;17:66–73.

7. Gass JDM, Blodi BA. Idiopathic Juxtafoveolar Retinal Telangiectasis: Update of Classification and Follow-up Study. Ophthalmology 1993;100:1536–1546.

8. Spaide RF, Yannuzzi LA, Maloca PM. Retinal-choroidal anastomosis in macular telangiectasia type 2. Retina 2018;38:1920–1929.

9. Meleth AD, Toy BC, Nigam D, et al. Prevalence and progression of pigment clumping associated with idiopathic macular telangiectasia Type 2. Retina 2013;33:762–770.

10. Leung I, Sallo FB, Bonelli R, et al. CHARACTERISTICS OF PIGMENTED LESIONS IN TYPE 2 IDIOPATHIC MACULAR TELANGIECTASIA. Retina 2018;38:S43–S50.

11. Gaudric A, Krivosic V, Tadayoni R. Outer retina capillary invasion and ellipsoid zone loss in macular telangiectasia type 2 imaged by optical coherence tomography angiography. Retina 2015;35:2300–2306.

12. Li ZY, Possin DE, Milam AH. Histopathology of Bone Spicule Pigmentation in Retinitis Pigmentosa. Ophthalmology 1995;102:805–816.

13. Milam AH, Li ZY, Fariss RN. Histopathology of the human retina in retinitis pigmentosa. Prog Retin Eye Res 1998;17:175–205.

14. Bonilha VL, Rayborn ME, Li Y, et al. Histopathology and functional correlations in a patient with a mutation in RPE65, the gene for retinol isomerase. Investig Ophthalmol Vis Sci 2011;52:8381–8392.

15. Goldberg MF, McLeod S, Tso M, et al. Ocular Histopathology and Immunohistochemical Analysis in the Oldest Known Individual with Autosomal Dominant Vitreoretinochoroidopathy. Ophthalmol Retin 2018;2:360–378.

16. Cao D, Leong B, Messinger JD, et al. Hyperreflective foci, optical coherence tomography progression indicators in age-related macular degeneration, include transdifferentiated

retinal pigment epithelium. Investig Ophthalmol Vis Sci 2021;62.

17. Balaratnasingam C, Messinger JD, Sloan KR, et al. Histologic and Optical Coherence Tomographic Correlates in Drusenoid Pigment Epithelium Detachment in Age-Related Macular Degeneration. Ophthalmology 2017;124:644–656.

18. Li M, Dolz-Marco R, Messinger JD, et al. Clinicopathologic Correlation of Anti–Vascular Endothelial Growth Factor–Treated Type 3 Neovascularization in Age-Related Macular Degeneration. Ophthalmology 2018;125:276–287.

19. Petty HR, Elner VM, Kawaji T, et al. A facile method for immunofluorescence microscopy of highly autofluorescent human retinal sections using nanoparticles with large Stokes shifts. J Neurosci Methods 2010;191:222–226.

20. Sall JW, Klisovic DD, O'Dorisio MS, Katz SE. Somatostatin inhibits IGF-1 mediated induction of VEGF in human retinal pigment epithelial cells. Exp Eye Res 2004;79:465–476.

21. Båvik CO, Lévy F, Hellman U, et al. The retinal pigment epithelial membrane receptor for plasma retinol-binding protein: Isolation and cDNA cloning of the 63-kDa protein. J Biol Chem 1993;268:20540–20546.

22. Hamel CP, Tsilou E, Pfeffer BA, et al. Molecular cloning and expression of RPE65, a novel retinal pigment epithelium-specific microsomal protein that is post-transcriptionally regulated in vitro. J Biol Chem 1993;268:15751–7.

23. Gan Z, Ding L, Burckhardt CJ, et al. Vimentin Intermediate Filaments Template Microtubule Networks to Enhance Persistence in Cell Polarity and Directed Migration. Cell Syst 2016;3:500–501.

24. Grisanti S, Guidry C. Transdifferentiation of retinal pigment epithelial cells from epithelial to mesenchymal phenotype. Investig Ophthalmol Vis Sci 1995;36:391–405.

25. Hunt RC, Davis AA. Altered expression of keratin and vimentin in human retinal pigment epithelial cells in vivo and in vitro. J Cell Physiol 1990;145:187–199.

26. Kalluri R, Weinberg RA. The basics of epithelial-mesenchymal transition. J Clin Invest 2009;119:1420–8.

27. Guidry C, Medeiros NE, Curcio CA. Phenotypic variation of retinal pigment epithelium in age-related macular degeneration. Investig Ophthalmol Vis Sci 2002;43:267–273.

28. Schamburg Lever G, Lever WF. Electron microscopy of incontinentia pigmenti. J Invest Dermatol 1973;61:151–158.

29. Weng YR, Cui Y, Fang JY. Biological functions of cytokeratin 18 in cancer. Mol Cancer Res 2012;10:485–493.

30. Fuchs U, Kivela T, Tarkkanen A. Cytoskeleton in normal and reactive human retinal pigment epithelial cells. Investig Ophthalmol Vis Sci 1991;32:3178–3186.

31. Grossniklaus HE, Ling JX, Wallace TM, et al. Macrophage and retinal pigment epithelium expression of angiogenic cytokines in choroidal neovascularization. Mol Vis 2002;8:119–26. Available at: http://www.ncbi.nlm.nih.gov/pubmed/11979237.

32. Kasper M, Moll R, Stosiek P, Karsten U. Patterns of cytokeratin and vimentin expression in the human eye. Histochemistry 1988;89:369–377.

33. Shepard JL, Zon LI. Developmental derivation of embryonic and adult macrophages. Curr Opin Hematol 2000;7:3–8.

34. Sheridan C, Hiscott P, Grierson I. Retinal Pigment Epithelium Differentiation and Dedifferentiation. In: *Vitreo-retinal Surgery*. Berlin/Heidelberg: Springer-Verlag; 2005:101–119.

35. Gass JDM. Focal congenital anomalies of the retinal pigment epithelium. Eye 1989;3:1–18.

36. Parsons MA, Rennie IG, Rundle PA, et al. Congenital hypertrophy of retinal pigment epithelium: A clinico-pathological case report [3]. Br J Ophthalmol 2005;89:920–921.

37. Lewis H, Straatsma BR, Foos RY, Lightfoot DO. Reticular Degeneration of the Pigment Epithelium. Ophthalmology 1985;92:1485–1495.

38. Shields JA, Tso MO. Congenital Grouped Pigmentation of the Retina. Histopathologic Description and Report of a Case. ArchOphthalmol 1975;93:1153.

39. Chen L, Li M, Messinger JD, et al. Recognizing atrophy and mixed-type neovascularization in age-related macular degeneration via clinicopathologic correlation. Transl Vis Sci Technol 2020;9:1–15.

40. Zanzottera EC, Messinger JD, Ach T, et al. Subducted and melanotic cells in advanced age-related macular degeneration are derived from retinal pigment epithelium. Investig Ophthalmol Vis Sci 2015;56:3269–3278.

41. Zanzottera EC, Messinger JD, Ach T, et al. The project macula retinal pigment epithelium grading system for histology and optical coherence tomography in age-related macular degeneration. Investig Ophthalmol Vis Sci 2015;56:3253–3268.

42. Tamiya S, Liu LH, Kaplan HJ. Epithelial-mesenchymal transition and proliferation of retinal pigment epithelial cells initiated upon loss of cell-cell contact. Investig Ophthalmol Vis Sci 2010;51:2755–2763.

43. Zhao C, Yasumura D, Li X, et al. mTOR-mediated dedifferentiation of the retinal pigment epithelium initiates photoreceptor degeneration in mice. J Clin Invest 2011;121:369–83.

44. Alge CS, Suppmann S, Priglinger SG, et al. Comparative proteome analysis of native differentiated and cultured dedifferentiated human RPE cells. Investig Ophthalmol Vis Sci 2003;44:3629–3641.

45. Chen KC, Jung JJ, Curcio CA, et al. Intraretinal Hyperreflective Foci in Acquired Vitelliform Lesions of the Macula: Clinical and Histologic Study. Am J Ophthalmol 2016;164:89–98.

46. Dunn KC, Aotaki-Keen AE, Putkey FR, Hjelmeland LM. ARPE-19, a human retinal pigment epithelial cell line with differentiated properties. Exp Eye Res 1996;62:155–170.

47. Boulton ME. Studying melanin and lipofuscin in RPE cell culture models. Exp Eye Res 2014;126:61–67.

Figures

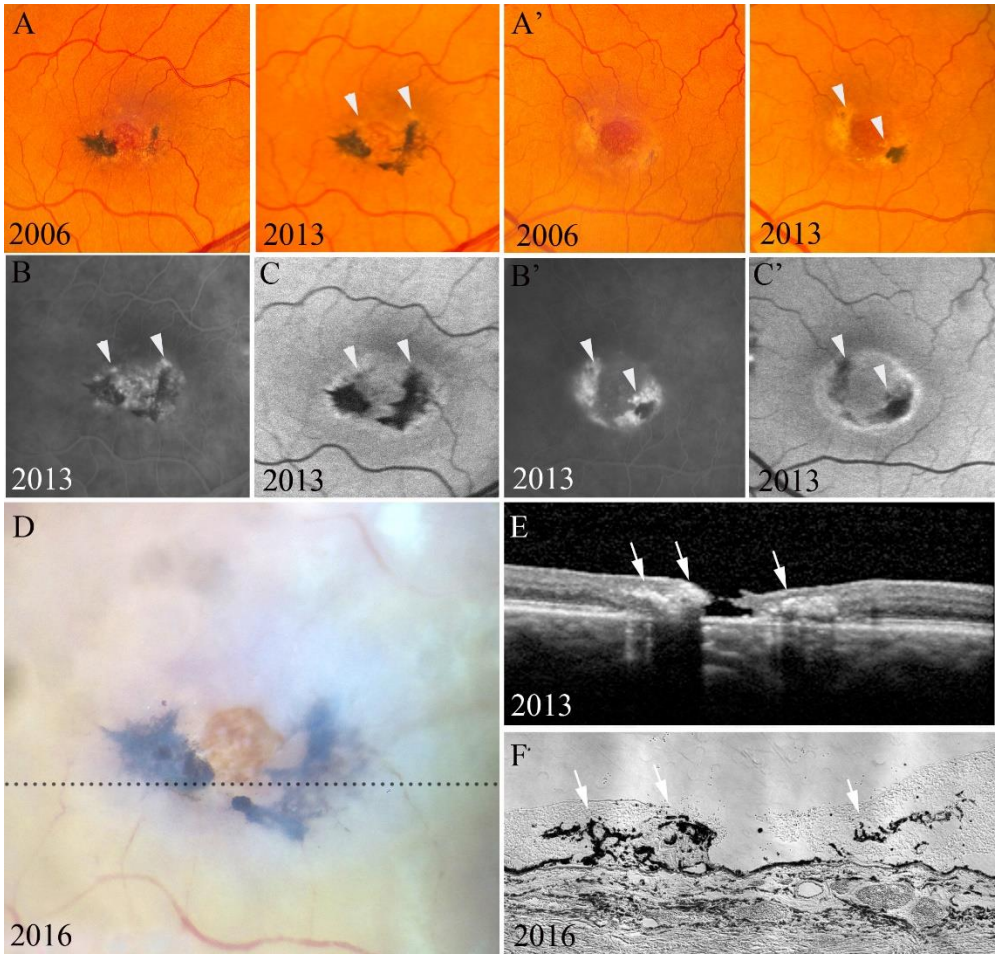

Figure 1. Clinical and histological presentation of MacTel case 1 in multiple imaging modalities. (**A**) Colour fundus photographs of the right and (**A'**) left macula (taken in 2006 and 2013) show typical features of the disease and their progression, such as telangiectatic vessel and pigmented plaques. (**B and B'**) In both eyes, late phase fluorescein angiography shows leakage in the macula. In addition, some distinct bright patches (arrowheads) can be attributed to a lack of RPE pigmentation or RPE cells, revealing the underlying choroid vasculature (window defect). (**C and C'**) In these locations (arrowheads), autofluorescent imaging shows dark grey patches (absence of autofluorescent RPE cells), which correspond to brighter patches in the colour fundus images. (**D**) A postmortem colour photograph of right eye shows melanin pigment plaques nasally and temporally of a macular hole (brown patch). (**E**) OCT imaging (roughly at the location of the stippled line in E) shows the macular hole and hyperreflective clusters (arrows). (**F**) A histological cryosection, matching the approximate location of the OCT b-scan, shows pigmented cell clusters (arrows) in similar locations as the hyperreflective clusters in the OCT.

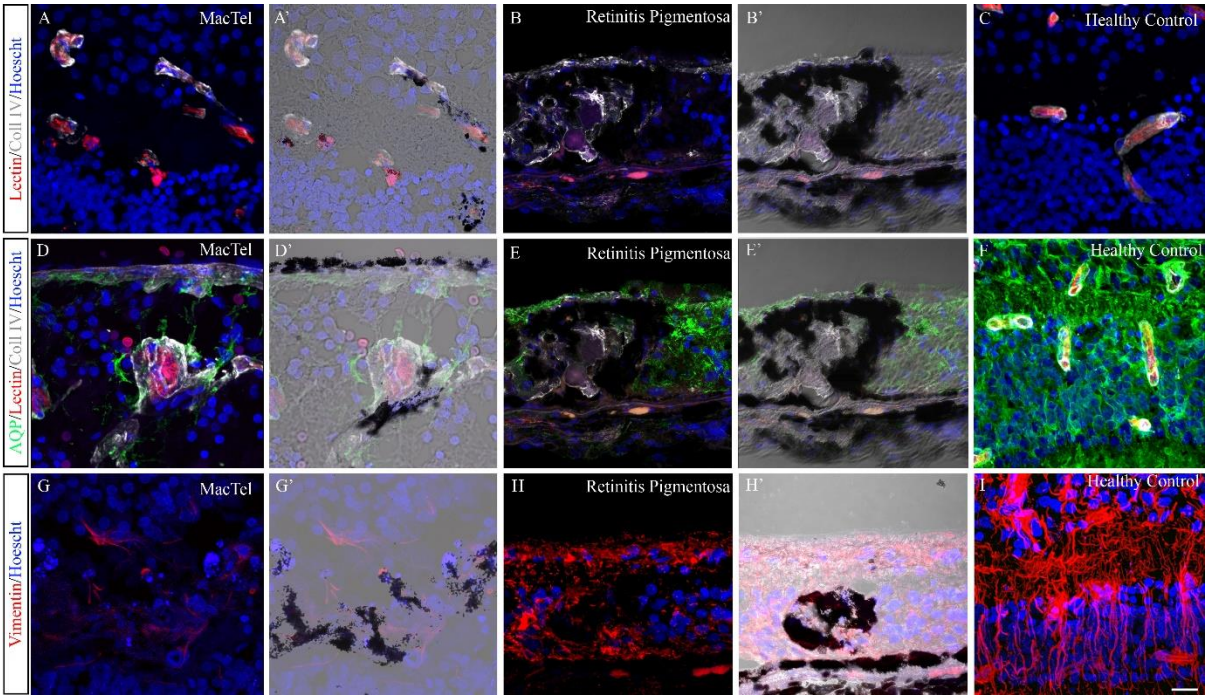

Figure 2. **Association of pigmented cells with blood vessels**. Sections from MacTel donor 1 (**A, A', D, D', G, G'**), a Retinitis Pigmentosa (RP) donor (**B, B', E, E', H, H'**) and a healthy control (**C, F, I**) were processed for immunofluorescence. Pigmented cells can be seen in the bright field overlays (**A', B', D', E' G', H'**) in the and are associated with blood vessels staining (**A-F**) in red (lectin stain) and white (collagen IV stain). Müller cells are shown in green (**D-F**, aquaporin-4 stain) and red (**G-I**, vimentin stain). Nuclei are shown in blue (labelled with Hoechst). Images were acquired with a 40X oil objective, scale bar is 20µm.

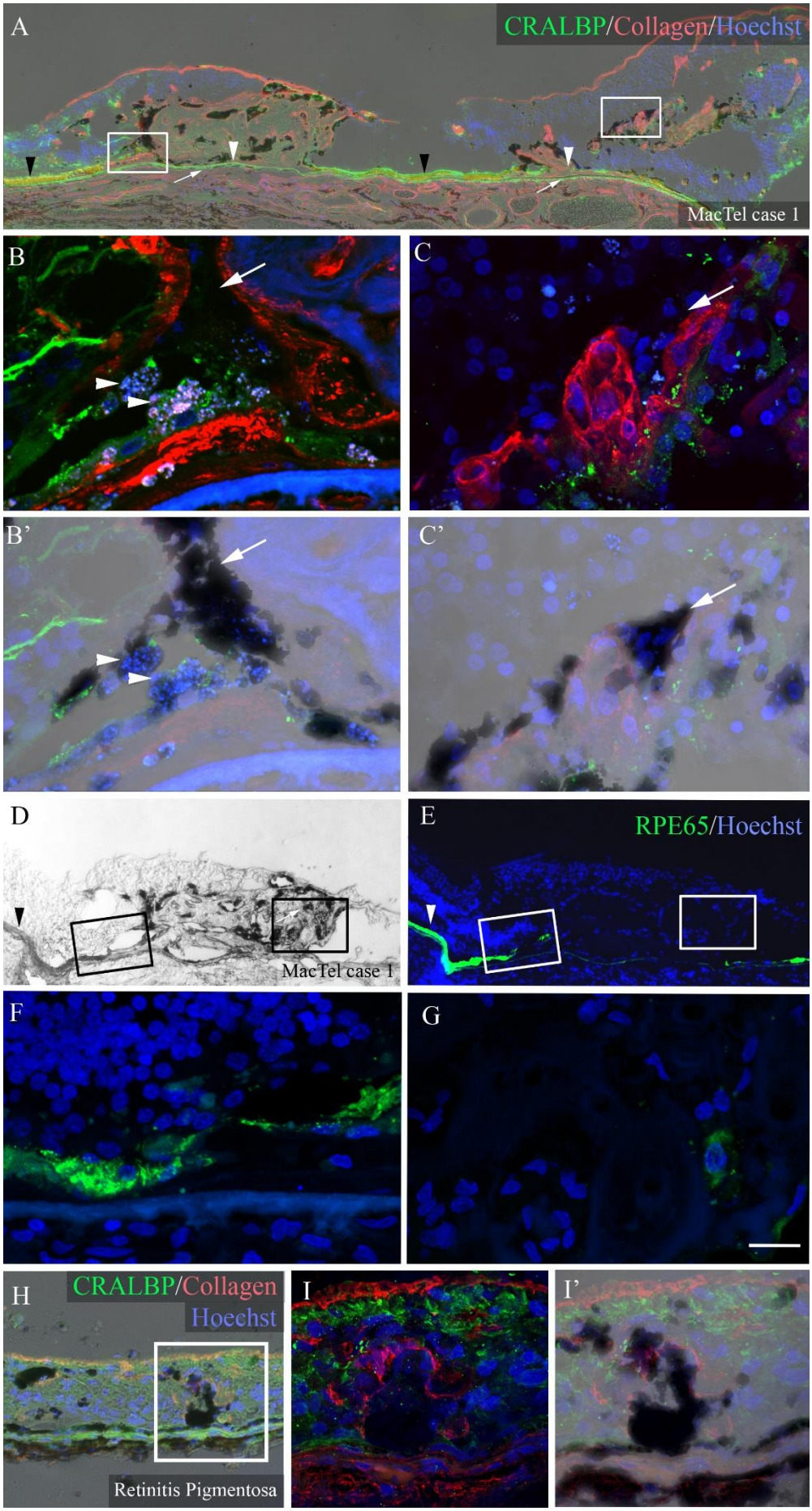
A
CRALBP/Collagen/Hoechst
MacTel case 1
B
C
B'
C'
D
MacTel case 1
E
RPE65/Hoechst
F
G
H
CRALBP/Collagen
Hoechst
Retinitis Pigmentosa
I
I'

Figure 3. Intraretinal pigmented cells do not express RPE markers. Brightfield overlays (**A, B', C', F, H, I'**) show the distribution of pigmented cells in a section from MacTel donor 1 (**A-G**) and a Retinitis Pigmentosa donor (**H-I'**), stained for the RPE markers (in green) CRALBP (**A-C'**, **F-I'**) and RPE65 (**D-G**), and the vascular marker collagen IV (**A-C'**, **F-I'**, red). The overview image of the MacTel case (**A**) shows intact RPE (black arrowheads) and areas where RPE cells are missing (white arrowheads) and only Bruch's membrane (white arrows in A) remains. Intraretinal CRALBP staining is associated with Müller cell remnants but absent from intraretinal pigmented cells. White boxes in A are magnified in B, B' (left box) and C, C' (right box), which reveal some residual CRALBP stain in cells containing lipofuscin granules (white arrowheads in B, B') but a complete absence of CRALBP in other pigmented cells (white arrows in B-C'). Similarly, RPE65 staining (**E-G**) is not visible in intraretinal pigmented cells either on a MacTel section where melanin bleaching was applied to ensure the fluorescent staining is not obscured (**D** shows the section before bleaching), whilst RPE cells are strongly labelled (arrowheads in **D, E**). Magnified views of boxes in D, E are shown in F, G. In the RP sample (**H-I'**), CRALBP staining is visible in gliotic Müller cells, but not intraretinal pigmented cells. The box in H is shown in I, I'. Nuclei are shown in blue (labelled with Hoechst). Panel A, D, E and H were imaged with a 20X objective, the rest are confocal images acquired with a 40X oil objective.

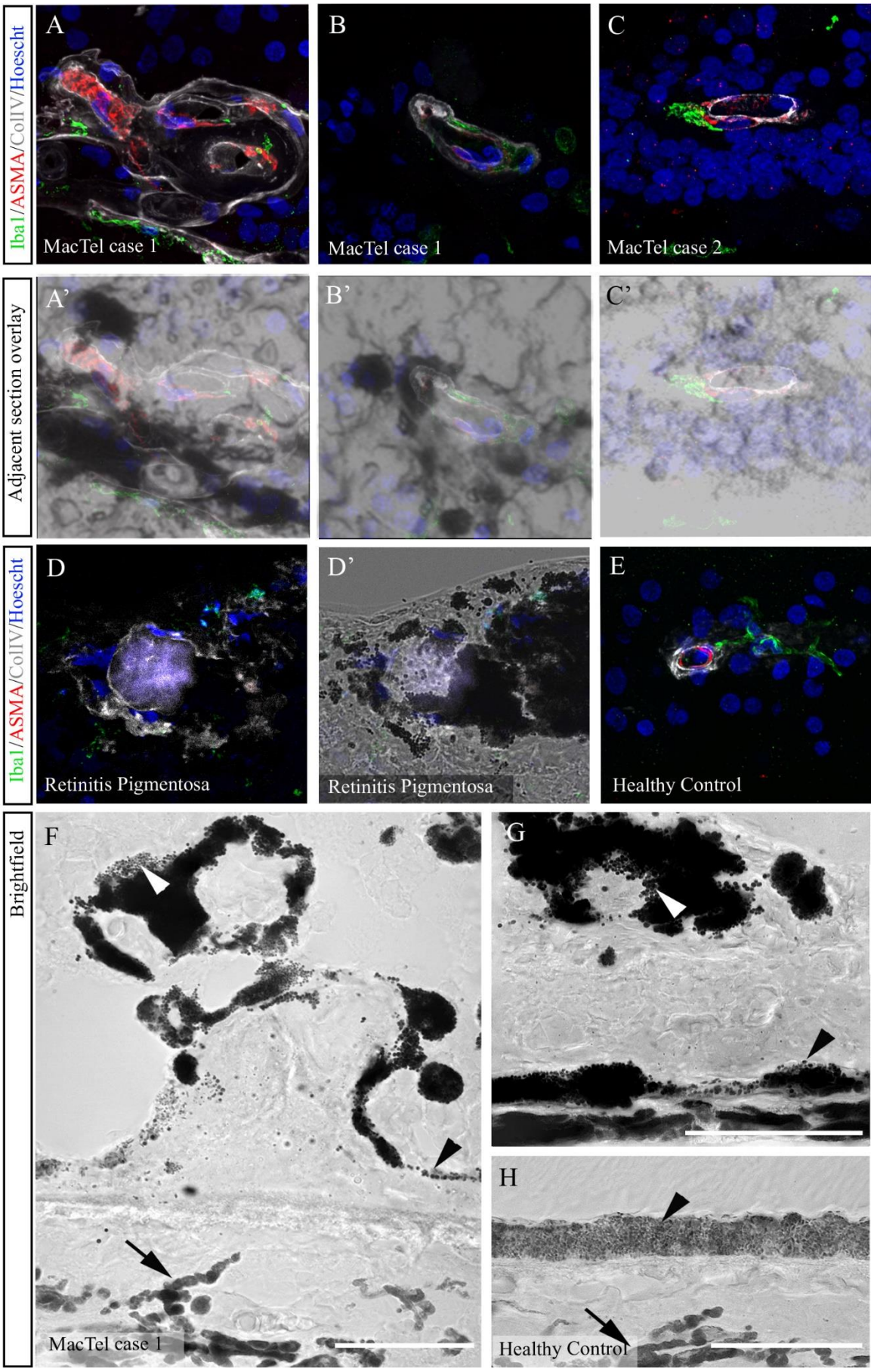
Iba1/ASMA/CollV/Hoescht
A
MacTel case 1
B
MacTel case 1
C
MacTel case 2
Adjacent section overlay
A'
B'
C'
Iba1/ASMA/CollV/Hoescht
D
Retinitis Pigmentosa
D'
Retinitis Pigmentosa
E
Healthy Control
Brightfield
F
MacTel case 1
G
H
Healthy Control

Figure 4. **Intraretinal pigmented cells are not mesenchymal or inflammatory cells or uveal melanocytes.** (**A-C**) Immunohistochemistry for IBA1 (green, inflammatory cells) and ASMA (red, marker for vascular smooth muscle cells and RPE cells undergoing EMT) in MacTel case 1, 2, Retinitis Pigmentosa shows in corresponding brightfield overlays (**A', B' C'**) that intraretinal pigmented cells are neither mesenchymal nor inflammatory in nature. Nuclei are shown in blue (labelled with Hoechst). Brightfield imaging of the MacTel (**F**), the Retinitis Pigmentosa (**G**) and the control (**H**) donor tissue shows large intracellular pigment granules in RPE (black arrowheads) and intraretinal pigmented cells (black arrowheads) of similar size in both cell types. In contrast, pigment granules in uveal melanocytes (black arrows) are much smaller and cannot to be individually discerned at the resolution shown. All confocal images were acquired with a 40X oil objective.

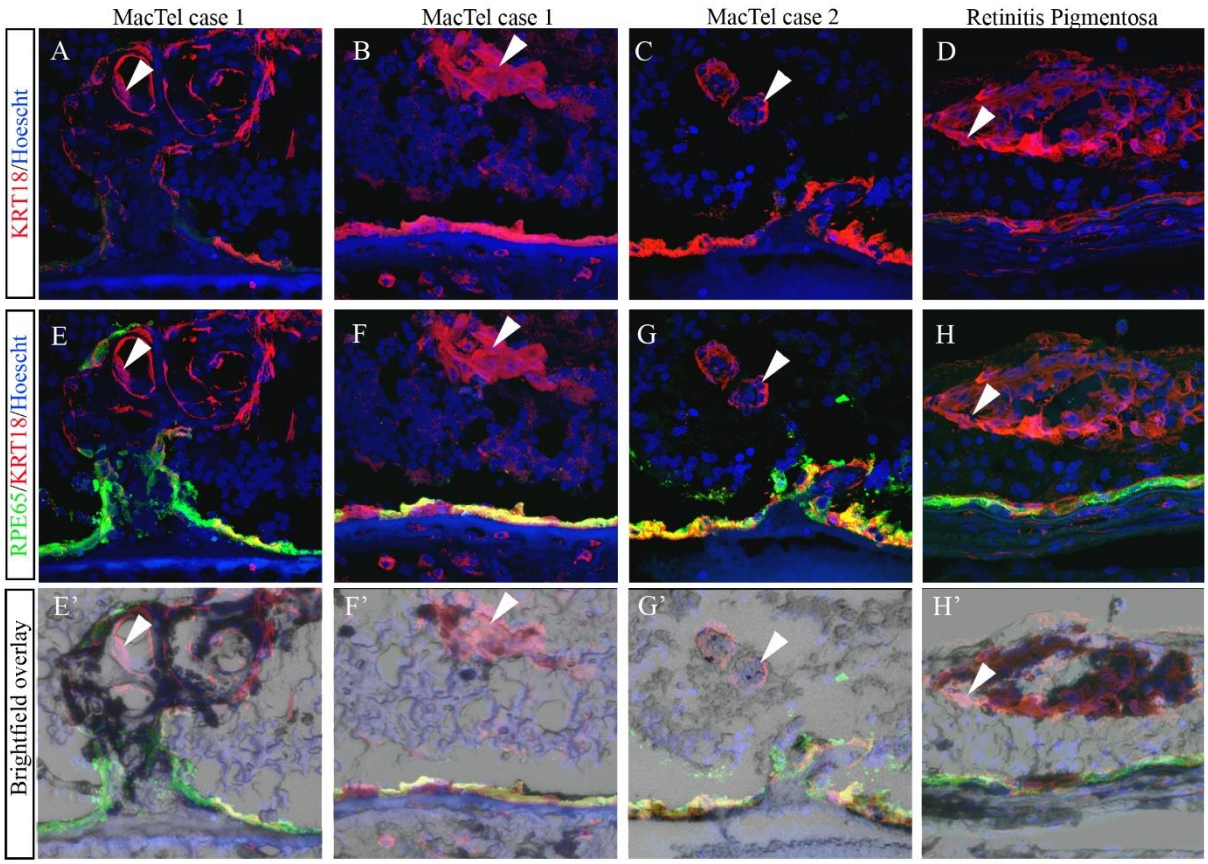

Figure 5. **Intraretinal pigmented cells express KRT18**. Immunostaining for KRT18 (**A-L**) and RPE65 (**E-L**) in MacTel donors 1, 2 (**A-C, E-G, E'-G'**) and a Retinitis Pigmentosa donor (**D, H, H'**) shows KRT18 labelling in RPE cells (RPE65 positive) and intraretinal pigment cells (arrowheads) visualised in brightfield overlays (**E'-H'**). Nuclei are shown in blue (labelled with Hoechst).

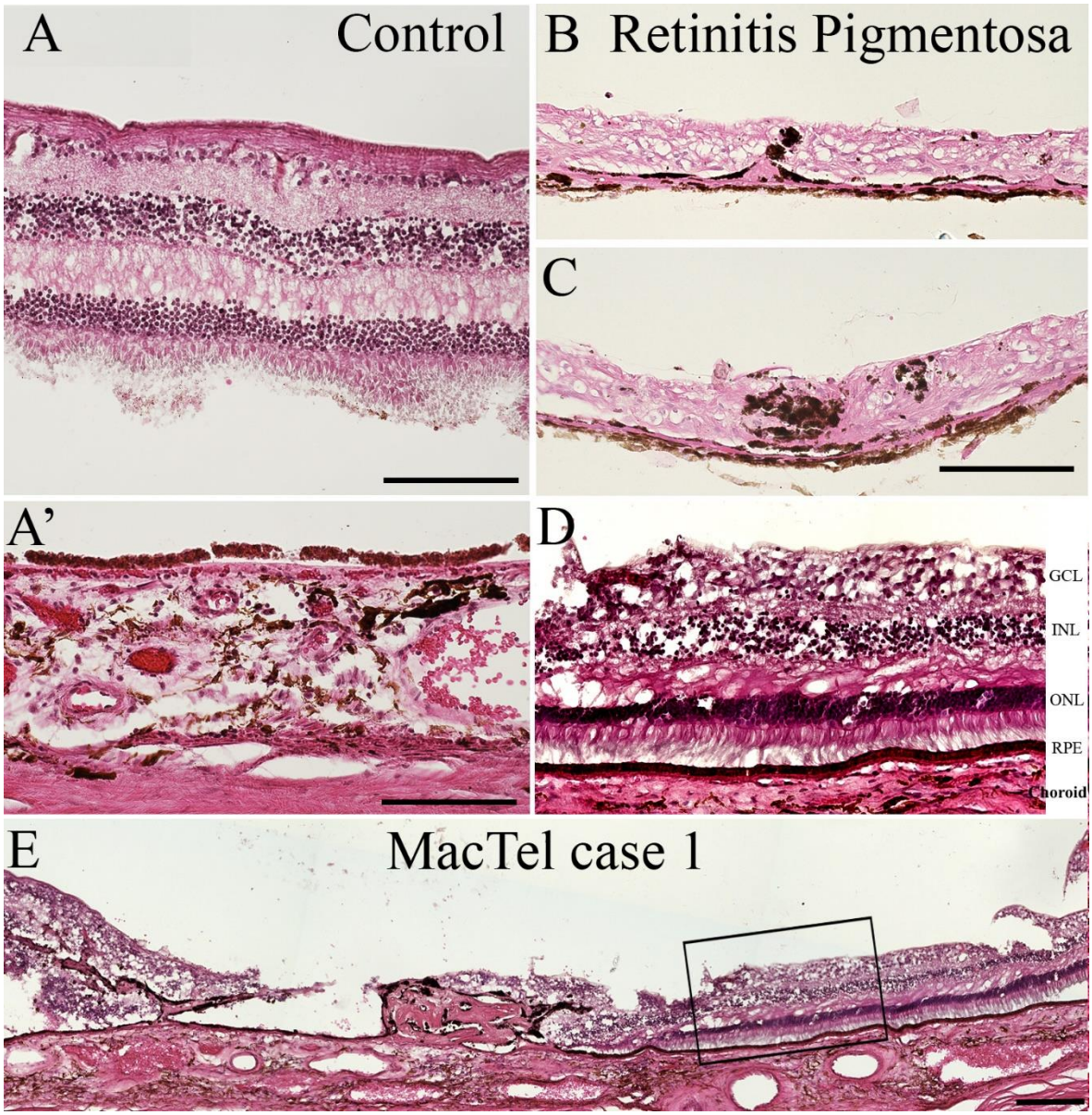

Supplemental figure 1. Haematoxylin and eosin (H&E) staining sections from the donor tissue used in this study. Representative sections are shown for one of the control donor's retina (A) and choroid/RPE (A'), the RP donor (B, C), and the MacTel case 1 (D, E). The box in E corresponds to D. All images were acquired with a 20x objective. Scale bars are 100µm